Separation Science and Technology
Publication details, including instructions for authors and subscription information:
http://www.tandfonline.com/loi/lsst20

Ordered Mesoporous Carbon CMK-3 Modified with Cu(I) for Selective Ethylene/Ethane Adsorption

Wen-Juan Jiang [a] , Lin-Bing Sun [a] , Yu Yin [a] , Xue-Lin Song [a] & Xiao-Qin Liu [a]
[a] State Key Laboratory of Materials-Oriented Chemical Engineering , College of Chemistry and Chemical Engineering, Nanjing University of Technology , Nanjing , China
Accepted author version posted online: 27 Nov 2012.Published online: 14 Mar 2013.

To cite this article: Wen-Juan Jiang , Lin-Bing Sun , Yu Yin , Xue-Lin Song & Xiao-Qin Liu (2013) Ordered Mesoporous Carbon CMK-3 Modified with Cu(I) for Selective Ethylene/Ethane Adsorption, Separation Science and Technology, 48:6, 968-976, DOI: 10.1080/01496395.2012.712600

To link to this article: http://dx.doi.org/10.1080/01496395.2012.712600

Separation Science and Technology, 48: 968–976, 2013

ISSN: 0149-6395 print/1520-5754 online
DOI: 10.1080/01496395.2012.712600

Taylor & Francis
Taylor & Francis Group

Ordered Mesoporous Carbon CMK-3 Modified with Cu(I) for Selective Ethylene/Ethane Adsorption

Wen-Juan Jiang, Lin-Bing Sun, Yu Yin, Xue-Lin Song, and Xiao-Qin Liu
State Key Laboratory of Materials-Oriented Chemical Engineering, College of Chemistry and Chemical Engineering, Nanjing University of Technology, Nanjing, China

Ordered mesoporous carbon CMK-3 was modified with cuprous chloride (CuCl) by a spontaneous thermal dispersion approach. A new kind of π-complexation adsorbent was thus obtained and characterized by X-ray diffraction, N_2 adsorption, and transmission electron microscopy. The results show that the mesostructure of CMK-3 is well preserved after the introduction of CuCl. In comparison with parent CMK-3, the selectivity of ethylene over ethane increases from 0.93 on CMK-3 to 2.67 on CuCl/CMK-3. All of the adsorption isotherms can be well fitted with the corresponding models. The fitting parameters along with the heat of adsorption demonstrate that the introduction of CuCl improve the interaction of ethylene with adsorbent apparently. The present adsorbents may provide useful candidates for the separation of ethylene and ethane as well as other alkene-containing systems.

Keywords π-complexation; ethylene adsorption; modification; ordered mesoporous carbon; selectivity

INTRODUCTION

Ethylene is one of the most important chemicals for the petrochemical industry. Similar to other unsaturated hydrocarbons, ethylene mainly comes from the gas mixture of petroleum catalytic cracking, which contains its saturated counterpart, namely ethane. The very close relative volatilities and similar molecular sizes of ethylene and ethane cause the difficulty in their separation. Currently, the large-scale separation process is distillation, which is regarded as one of the most energy-intensive industrial process. Alternatively, several methods have been developed for alkene/alkane separation, such as adsorption, absorption, and membrane separation (1–5). Adsorption technology has been judged to be a promising candidate due to its low energy consumption and inexpensive equipment investment (6,7). Among diverse materials employed for adsorptive separation process (8–15), π-complexation adsorbents attract great interest due to the high selectivity (16–18). The selective adsorption of π-complexation adsorbents were achieved by their bonds stronger than the Van der Waals forces alone. The formation of π-complexes between alkene molecules and active sites (for example, Cu(I) and Ag(I)) has been proven to be a crucial step for the selective adsorption (19–21).

Various adsorbents have been tried for the adsorptive separation of ethylene and ethane (22–26). Anson et al. (24) prepared adsorbents derived from EST-10 zeolite exchanged with different cations. The adsorption capacity of ethylene and ethane on Ag-EST-10 is 1.12 and $1.01\,mmol \cdot g^{-1}$, respectively, corresponding to the selectivity of 1.12. Similar adsorption capacity of ethylene ($0.97\,mmol \cdot g^{-1}$) and ethane ($0.72\,mmol \cdot g^{-1}$) is obtained on Cu-EST-10. Chen et al. (25) incorporated copper into mesoporous silica MCM-48 for ethylene/ethane separation. Under the conditions of 1 atm and 30°C, the adsorption capacity of ethylene varied from 0.3 to $0.5\,mmol \cdot g^{-1}$ on Cu-MCM-48 with different copper content. Recently, He et al. (26) employed a metal-organic framework, UTSA-33, for the adsorption of ethylene and ethane. Their results show that the adsorption of ethylene and ethane on UTSA-33 is quite similar (about $2.6\,mmol \cdot g^{-1}$), indicative of a low selectivity. Despite many attempts, development of an adsorbent with high capacity and selectivity remains an open question up to now.

Due to their high surface areas, large pore volumes, and tunable pore structures, mesoporous materials are preferred choice of support for the dispersion of π-complexation adsorption active species. Less attention has been paid to mesoporous carbon. Mesoporous carbon has found applications in a variety of fields including catalysis, gas storage, electrochemical capacitance, as well as liquid adsorption (27–36). It is known that mesoporous carbon possesses an extremely high surface area (even larger than mesoporous silica), which is beneficial to the dispersion of active species. Moreover, the nature of reducibility on carbon surface may provide a special microenvironment to stabilize active sites such as Cu(I) for

Received 22 March 2012; accepted 12 July 2012.
Address correspondence to Xiao-Qin Liu, State Key Laboratory of Materials-Oriented Chemical Engineering, College of Chemistry and Chemical Engineering, Nanjing University of Technology, Nanjing 210009, China. Tel.: +86-25-83587178; Fax: +86-25-83587191. E-mail: liuxq@njut.edu.cn

π-complexation adsorption. Therefore, mesoporous carbon should be a promising candidate for applications in π-complexation adsorption.

In the present study, we reported the synthesis of a new π-complexation adsorbent by use of mesoporous carbon CMK-3 as the support and CuCl as the active component. Cuprous chloride was introduced to CMK-3 by solid-state grinding and subsequently thermal dispersion. The effects of temperature and time for thermal treatment on the dispersion of CuCl were investigated. By optimizing the preparation conditions, Cu(I)-modified mesoporous carbon with ordered structure and dispersed active species was obtained for the first time. The adsorbents were characterized by various methods including X-ray diffraction (XRD), N_2 adsorption, and transmission electron microscopy (TEM). Adsorption behavior of ethylene and ethane over these materials was investigated at different temperatures. On the basis of the experimental results, the adsorption data were fitted by different models for different adsorbates, and the mechanism for selective adsorption was discussed as well.

EXPERIMENTAL SECTION

Adsorbents Preparation

Mesoporous silica SBA-15 was synthesized according to the procedure reported by Zhao et al. (37). The chemical composition of synthetic mixture was 4 g triblock copolymer P123 ($EO_{20}PO_{70}EO_{20}$) : 0.0405 mol tetraethylorthosilicate (TEOS) : 0.24 mol HCl : 8 mol H_2O. The clear solution was stirred at 35°C for 24 h followed by hydrothermal reaction at 100°C for 24 h. The product was recovered by filtration, washed with water, and calcined in air at 550°C for 5 h.

The mesoporous carbon CMK-3 was prepared by using mesoporous silica SBA-15 as the template and sucrose as the carbon source. In a typical synthesis (38), 1 g of SBA-15 was added to a solution obtained by dissolving 1.25 g of sucrose and 0.14 g of H_2SO_4 in 5 g of H_2O. The mixture was heated to 100°C and kept at the temperature for 6 h. Subsequently, the temperature was enhanced to 160°C for another 6 h. To obtain fully polymerized and carbonized sucrose inside the pores, 0.8 g of sucrose, 0.09 g of H_2SO_4, and 5 g of H_2O were added to the pretreated sample again and the mixture was treated as described above. The template-polymer composite was then carbonized at 900°C for 6 h with a heating rate of $5°C \cdot min^{-1}$ under flowing nitrogen. The silica template was removed using 1 M NaOH solution (50 vol% ethanol-50 vol% H_2O) at 80°C. The obtained carbon product was filtered, washed with water, and dried at 100°C.

The active component CuCl was incorporated into CMK-3 by solid-state grinding. About 0.4 or 0.8 mmol (0.04 or 0.08 g) CuCl was manually ground with 0.1 g CMK-3 for 10 min, leading to the formation of 0.14–0.18 g sample each time. The resultant powder was thermally treated in a nitrogen flow at a certain temperature. The obtain material was denoted as *n*CuCl/CMK-3, where *n* represents the millimole of cuprous chloride in per gram of CMK-3.

Characterization

XRD patterns of the materials were recorded using a Bruker D8 Advance diffractometer with Cu Kα radiation in the 2θ range from 0.5° to 8° and 10° to 80° at 40 kV and 40 mA. The N_2 adsorption-desorption isotherms were measured using a BLSORP II system at −196°C. The samples were degassed at 200°C for 4 h prior to analysis. The Brunauer-Emmett-Teller (BET) surface area was calculated using adsorption data in a relative pressure range from 0.04 to 0.20. The total pore volume was determined from the amount adsorbed at a relative pressure of about 0.99. The pore diameter was calculated from the adsorption branch by using the Barrett-Joyner-Halenda (BJH) method. TEM analysis was performed on a JEM-2010 UHR electron microscope operated at 200 kV.

Adsorptive Test and Analysis

Pure ethane and ethylene adsorption isotherms were measured using an intelligent gravimetric analyzer (IGA-100) supplied by Hiden Analytical, Ltd. The microbalance had a long-term stability of ±1 μg with a weighing resolution of 0.2 μg. The sample ($<100 \pm 1$ mg) was outgassed until it reached a constant weight, at a pressure of $<10^{-6}$ Pa at 200°C prior to measurement. The pressure was then increased gradually, over a period of 60 s, to the desired pressure, in order to prevent disruption of the balance. The sample was heated to the experimental temperatures by use of water bath or furnace.

In the analysis of adsorption equilibrium, the adsorption of ethane includes only physical adsorption that can be described well by the Langmuir model as shown in Eq. (1).

$$q = \frac{q_{mp} b_p P}{1 + b_p P} \tag{1}$$

However, the adsorption of ethylene on CuCl/CMK-3 includes both physical and chemical adsorption. The model should fully consider the energetic heterogeneity of surface ion sites for chemisorptions (39). Therefore, a model combining the physical adsorption with the chemical one is adapted and shown in Eq. (2).

$$q = \frac{q_{mp} b_p P}{1 + b_p P} + \frac{q_{mc}}{2s} \ln \frac{1 + b_c P e^{s}}{1 + b_c P e^{-s}} \tag{2}$$

where subscripts p and c indicate physical adsorption and chemisorptions. q_{mp} and q_{mc} are the maximum adsorbed

phase concentrations of physical adsorption and chemisorption; b_p and b_c are the physical adsorption and chemisorptions constant, respectively; s is a heterogeneity parameter indicating the spread of energy distribution.

This description of the adsorption equilibrium contains five parameters and their values are obtained from the experimental isotherm data by nonlinear regression. Certain constraints must be imposed on some of the parameters in order for them to have physical meaning. The value for s is available from the "Adsorption Equilibrium Data Handbook" (40), and generally falls within the range 0–7. The Marquardt nonlinear regression method was used. For each sorbent, the ethane data were used to obtain the two parameters of the Langmuir isotherm (q_{mp} and b_p). For each π-complexation adsorbent, Eq. (2) was used to fit the ethylene adsorption data with the corresponding two parameters obtained in the Langmuir equation, leaving only q_{mc} and b_c as true fitting parameters.

In addition, the isosteric heats of adsorption were evaluated using the Clausius-Clapeyron equation shown in Eq. (3).

$$\left[\frac{\partial \ln P}{\partial(1/T)}\right]_q = \frac{-\Delta H}{R} \tag{3}$$

where $-\Delta H$ is the isosteric heat of adsorption, P is the equilibrium pressure at the temperature T, and R is the universal gas constant. We used the fitting curves instead of experimental ones to simulate the dependency of P from $1/T$.

The selectivity of ethylene over ethane on different adsorbents is calculated via Eq. (4).

$$S_{ij} = \frac{x_i/x_j}{y_i/y_j} \tag{4}$$

where x_i and x_j are the equilibrated adsorption capacity of ethylene and ethane respectively, and y_i and y_j are the molar fractions of ethylene and ethane in gas phases respectively.

RESULTS AND DISCUSSION

Effect of Thermal Treatment Conditions on CuCl Dispersion

In general, CuCl can be dispersed on the surface of supports spontaneously if subjected to thermal treatment for several hours at the temperatures adjacent its melting point (430°C) (41,42). Thus, the effect of temperature is first investigated. Figure 1 shows the wide-angle XRD patterns of 8CuCl/CMK-3 samples thermally treated at different temperatures. For the sample treated at 250°C, three major diffraction peaks at 28.5°, 47.5°, and 56.3° with a minor one at 33.0° are observable; these peaks can be ascribed to CuCl (JCPDS No. 06-0344). When the treatment temperature increased to 300°C, the intensity of diffraction peaks decreased obviously, indicative of an improved dispersivity. It is noticeable that two new peaks at 43.3° and 50.5° appear on the sample treated at 350°C. This means that metallic copper (JCPDS No. 65-9026) is produced from the reaction of CuCl with carbon support at the elevated temperature. Because the ion pairs or molecules move faster from the surface of crystalline substance to the support at a higher temperature, CuCl can be dispersed better at 300°C as compared with the case at 250°C. From the thermodynamic point of view, dispersive particles are much smaller than the crystalline CuCl, and its large surface energy directly affect thermodynamic stability, which favors the reaction between CuCl and support at a high temperature. Effect of time on CuCl dispersion was also investigated. However, prolonging the treatment time does not further promote the dispersion of CuCl in the present study. That means that the employed time is enough for CuCl to reach its optimum dispersivity on CMK-3. As a result, thermal treatment at 300°C for 4 h is appropriate for CuCl/CMK-3 samples, since only CuCl crystalline phase with low intensity is observed.

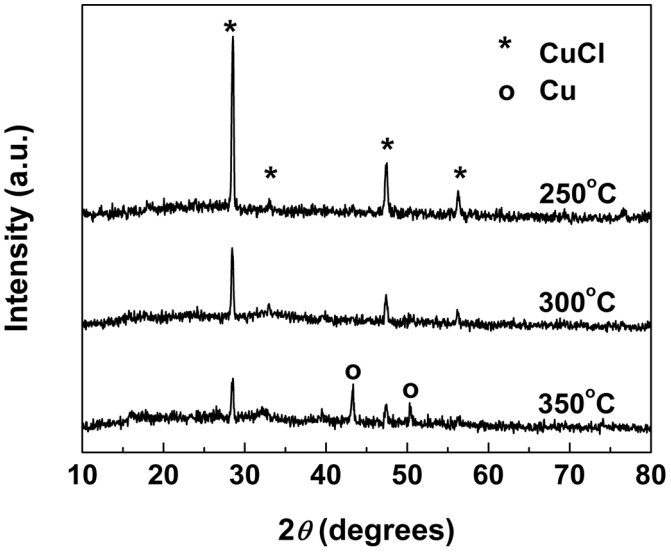

FIG. 1. Wide-angle XRD patterns of 8CuCl/CMK-3 treated at different temperatures.

Properties of Adsorbents

The low-angle XRD patterns of mesoporous silica SBA-15, mesoporous carbon CMK-3, and CuCl/CMK-3 samples are shown in Fig. 2a. The high intensity and good resolution of diffraction peaks indicate the long-distance ordered arrangement of hexagonal pore structure in SBA-15 and CMK-3 materials, similar to what reported in literature (36,37). After introducing CuCl, the position

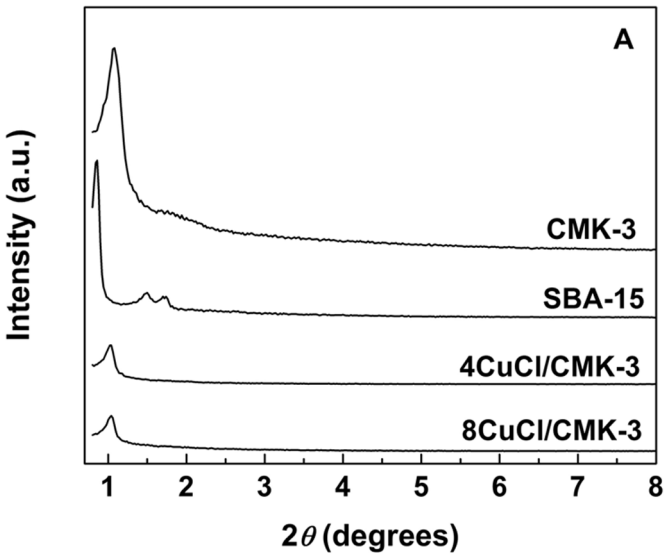

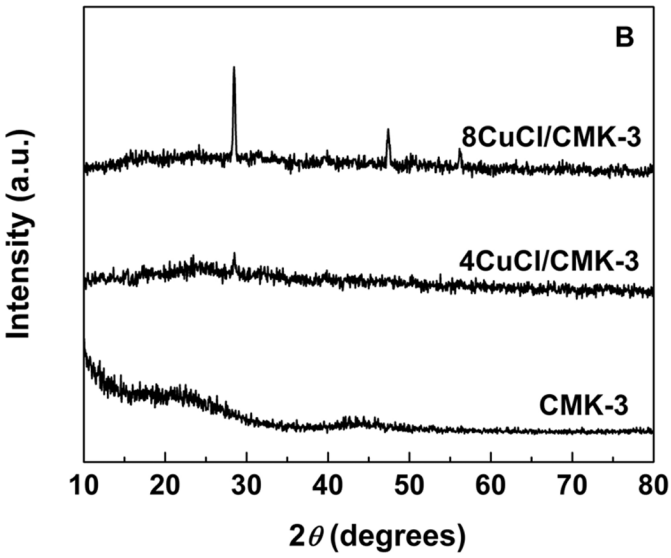

FIG. 2. (A) Low-angle and (B) wide-angle XRD patterns of SBA-15, CMK-3, and CuCl/CMK-3 samples.

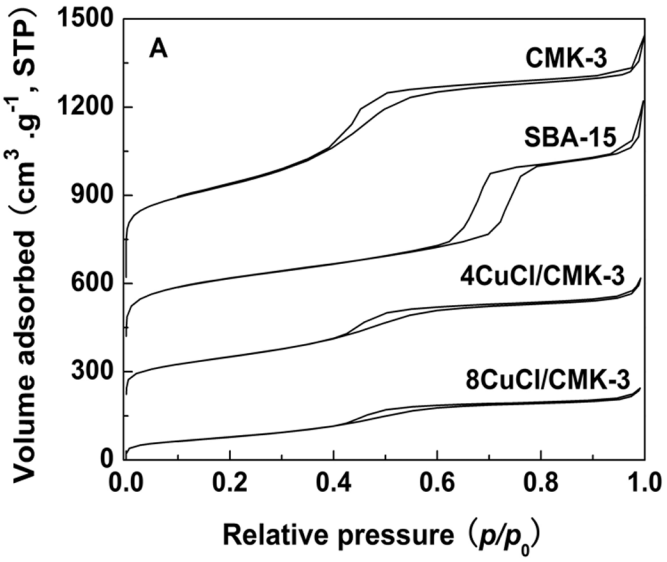

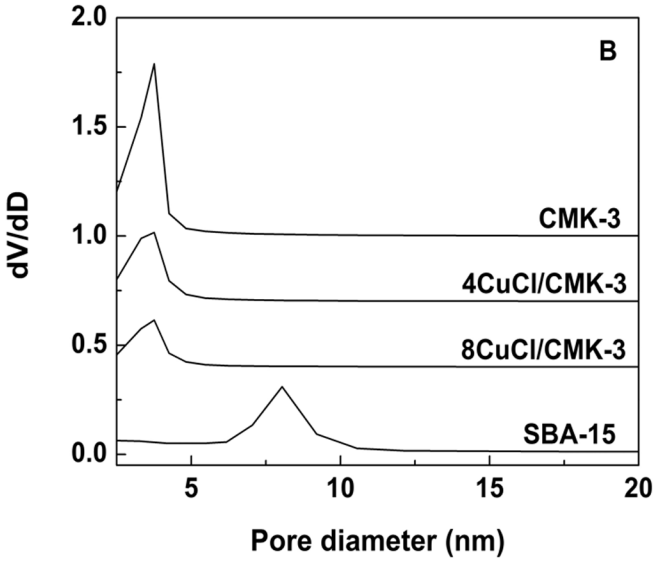

FIG. 3. (A) N_2 adsorption-desorption isotherms and (B) pore size distributions of SBA-15, CMK-3, and CuCl/CMK-3. Curves of 4CuCl/CMK-3, SBA-15, and CMK-3 in FIG. A are plotted offset by 200, 400, and 600 cm^3/g, respectively, while curves of 8CuCl/CMK-3, 4CuCl/CMK-3, and CMK-3 in Figure B are plotted offset by 0.4, 0.75, and 1.1, respectively.

of diffraction peaks keeps constant while the intensity decreases, as compared with parent CMK-3. The wide-angle XRD pattern of parent CMK-3 presents two broad diffraction line centered at 23° and 45° assigned to amorphous carbon (Fig. 2b). For the samples containing CuCl, characteristic diffraction peaks of CuCl crystallites become visible. Moreover, the intensity of diffraction peaks in 8CuCl/CMK-3 is higher than that in 4CuCl/CMK-3. These results demonstrate that CuCl have been successfully introduced to mesoporous carbon CMK-3.

Figure 3a depicts the N_2 adsorption-desorption isotherms of SBA-15 as well as CMK-3 before and after CuCl modification. CMK-3-related samples show an augment in adsorption at the relative pressure (p/p_0) of 0.4–0.8, which is different from the template SBA-15. Due to the loading of CuCl, the N_2 uptake decreases as compared with unmodified CMK-3. These results of N_2 adsorption are consistent with those of XRD described above. The BET surface areas and pore volumes were also calculated and listed in Table 1. The BET surface area of CMK-3 is 1182 $m^2 \cdot g^{-1}$ with a pore volume of 1.19 $cm^3 \cdot g^{-1}$, which is in good agreement with previous reports (40). For CuCl/CMK-3

TABLE 1
Textural properties and equilibrium selectivity of ethylene/ethane at 1 atm for different samples

Sample	S_{BET} ($m^2 \cdot g^{-1}$)	V_p ($cm^3 \cdot g^{-1}$)	Adsorption selectivity $q(C_2H_4)/q(C_2H_6)$ 30°C	50°C	70°C
SBA-15	782	1.11	–	–	–
CMK-3	1182	1.19	0.93	0.88	0.87
4CuCl/CMK-3	561	0.62	1.84	1.68	1.55
8CuCl/CMK-3	303	0.37	2.67	2.30	2.11

samples, both surface areas and pore volumes decrease gradually with the increase of CuCl content.

TEM provides another important technique to characterize the long-range channel ordering. TEM images of SBA-15, CMK-3, and 8CuCl/CMK-3 were shown in Fig. 4. The structure of CMK-3 carbon is a reverse copy of SBA-15. The carbon nanorods are interconnected by the carbon that filled the channel interconnecting micropores within the SBA-15 wall. The ordered hexagonal arrays of mesopores with uniform pore size and wall thickness can be judged from the white-dark contrast. These results demonstrate that the introduction of CuCl does not deteriorate the ordered mesoporous structure of CMK-3.

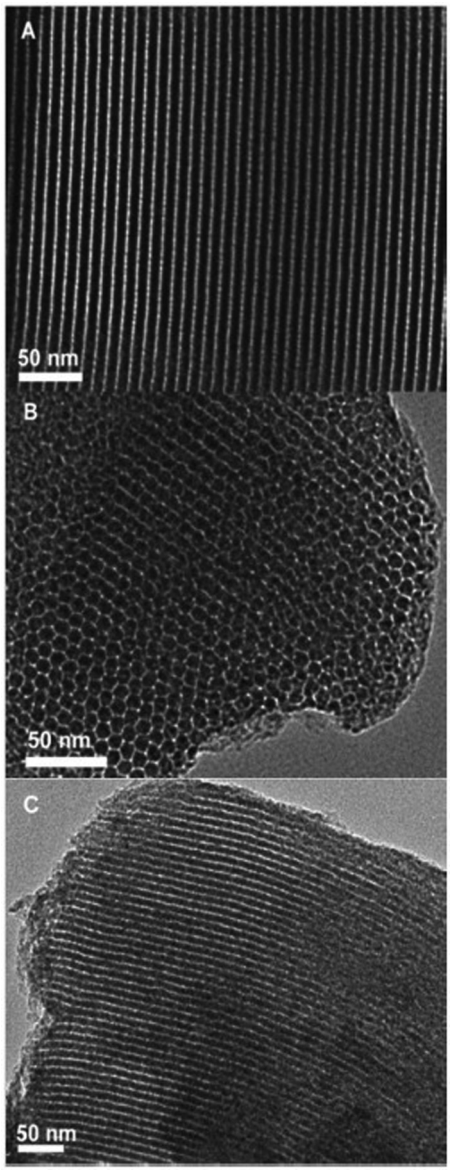

FIG. 4. TEM images of (A) SBA-15, (B) CMK-3, and (C) 8CuCl/CMK-3.

Adsorption Behavior

The adsorption performance of the obtained adsorbents on ethylene and ethane was investigated at three temperatures, that is, 30, 50, and 70°C. Figures 5–7 give the adsorption isotherms for CMK-3, 4CuCl/CMK-3, and 8CuCl/CMK-3, respectively. Unmodified CMK-3 shows a similar uptake for ethylene and ethane. For example, 1 g of CMK-3 can adsorb 2.88 mmol of ethylene and 3.11 mmol of ethane at 1 atm and 30°C, corresponding to a low equilibrium selectivity $q(C_2H_4)/q(C_2H_6)$ of 0.93 (Table 1). It is worth noting that the introduction of CuCl leads to the increase of ethylene uptake and the drop of ethane uptake. As shown in Fig. 6, the uptake of ethylene reaches 3.18 $mmol \cdot g^{-1}$ over 4CuCl/CMK-3, and that of ethane is only 1.73 $mmol \cdot g^{-1}$ at 1 atm and 30°C. As a result, the selectivity of ethylene over ethane increases to 1.84. Interestingly, further increasing the loading of CuCl on CMK-3 results in a more preferential adsorption of ethylene (3.55 $mmol \cdot g^{-1}$) over ethane (1.33 $mmol \cdot g^{-1}$), and the selectivity is almost triple (2.67) on 8CuCl/CMK-3 as compared with the parent CMK-3. The different adsorption behavior of ethylene and ethane can be attributed to different surface properties of CMK-3 before and after CuCl modification. There are only physical adsorption sites on unmodified CMK-3, and no special interaction existed between adsorbates and adsorbent. As a result, the uptake for ethylene and ethane is similar on CMK-3. The dispersion of CuCl generates some adsorption active sites on CMK-3 and increases the energetic heterogeneity of the surface. These newly generated Cu(I) sites can selectively interact with the C=C bond in ethylene through π-complexation, so the uptake of ethylene is enhanced. In the meanwhile, the original physical adsorption sites on CMK-3 are covered by CuCl, which leads to the decrease of ethane uptake. Furthermore, the more CuCl is introduced, the less physical adsorption sites will remain. As a

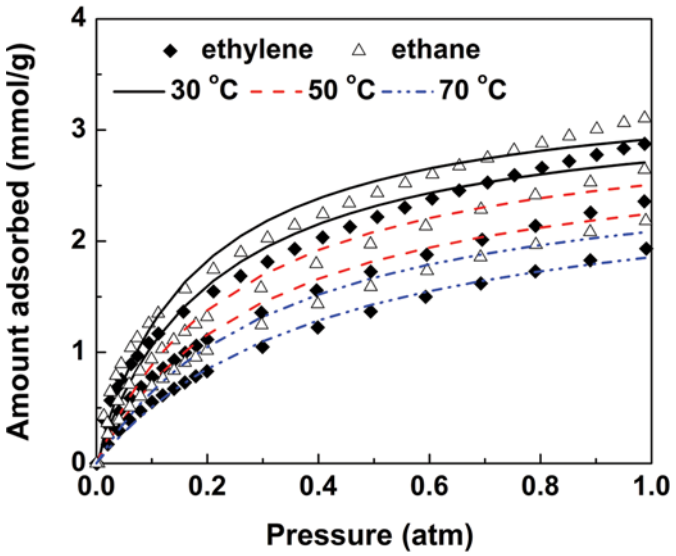

FIG. 5. Adsorption equilibriums of Ethylene and Ethane on CMK-3 at various temperatures. The lines are fitted results by use of corresponding models. (Color figure available online)

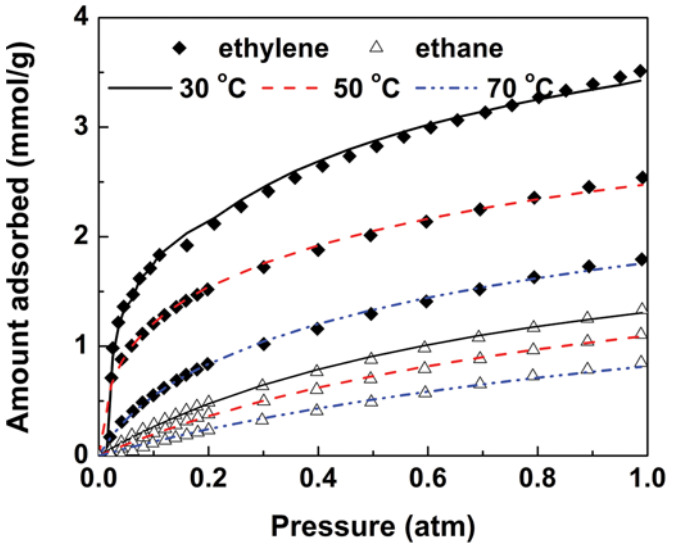

FIG. 7. Adsorption isotherms of Ethylene and Ethane on 8CuCl/CMK-3 at various temperatures. The lines are fitted results by use of corresponding models. (Color figure available online)

result, the CuCl-modified CMK-3 samples exhibit a selective adsorption of ethylene over ethane, and the selectivity increases with the increase of CuCl content.

To further understand the adsorption behavior, the aforementioned adsorption data were analyzed by nonlinear regression approach using the models described in Eqs. (1) and (2). For meaningful correlation using Eq. (2), physically reasonable constraints on the parameters are imposed. For physical adsorption, the values of the Langmuir constant (b_p) are approximately equal between ethylene and ethane with the same carbon number. The b value from the ethane isotherm is imposed as the upper bound for the corresponding ethylene. In addition, Cu(I) covers part of CMK-3 surface, and leave the residual surface intact. The Cu(I) sites are for the π-complexation with ethylene, whereas the unmodified sites are for physical adsorption of ethane. Knowing the extent of Cu(I) modified, q_{mp} and q_{mc} can be related. The parameters and curves derived from fitting are shown in Table 2 and Figs. 5–7. The ethane data can be well fitted by the two-parameter Langmuir isotherm. The fitted values for q_{mc} and b_c are both higher than their analogues from physical adsorption, indicative of a reasonable fitting. The b_c value is an indication for the bonding strength. As shown in Table 2, the parameters b_c of 8CuCl/CMK-3 adsorbent are higher than those of 4CuCl/CMK-3. That means the interaction between the adsorbate and the adsorbent on 8CuCl/CMK-3 is stronger than that on 4CuCl/CMK-3, which will be confirmed by the heat of adsorption as discussed later. The model constant s, which represents the energetic heterogeneity of a solid surface, increases with the Cu(I) content. The equilibrium isotherm of ethylene on 8CuCl/CMK-3 adsorbent is steeper than that on 4CuCl/CMK-3, so the values for s are higher and reasonable. This demonstrates that the introduction of active component does tailor the surface nature of support.

Figure 8 presents isosteric heat of adsorption for ethylene and ethane on different adsorbents as a function of uptake. The adsorption of ethane and ethylene on different adsorbents is the exothermic process. The dependence of heats of adsorption of ethane on adsorption coverage is not significant. The same trend of heat of adsorption for

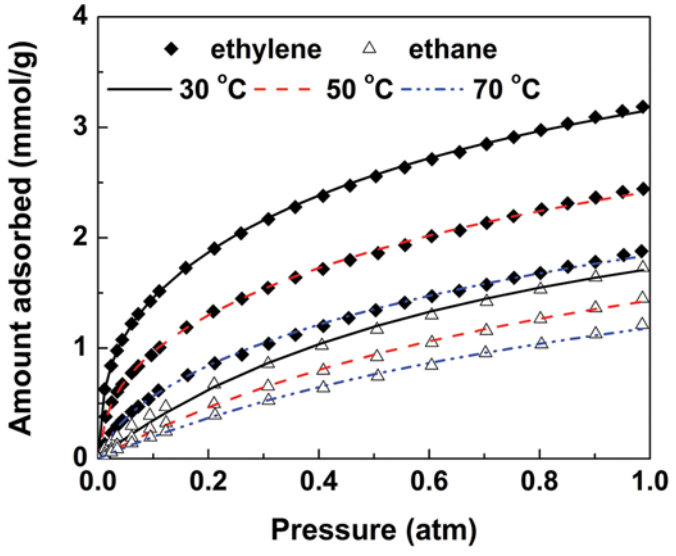

FIG. 6. Adsorption equilibriums of Ethylene and Ethane on 4CuCl/CMK-3 at various temperatures. The lines are fitted results by use of corresponding models. (Color figure available online)

TABLE 2
Parameters of adsorption isotherm for ethylene and ethane

Sample	T (°C)	Adsorbate	q_{mp} (mmol · g^{-1})	b_p (atm^{-1})	q_{mc} (mmol · g^{-1})	b_c (atm^{-1})	s
CMK-3	30	C_2H_4	3.28	4.74	–	–	–
		C_2H_6	3.43	5.68	–	–	–
	50	C_2H_4	2.94	3.26	–	–	–
		C_2H_6	3.15	3.89	–	–	–
	70	C_2H_4	2.64	2.38	–	–	–
		C_2H_6	2.78	3.02	–	–	–
4CuCl/CMK-3	30	C_2H_4	2.02	1.49	3.12	3.22	4.81
		C_2H_6	2.82	1.49	–	–	–
	50	C_2H_4	1.99	1.03	2.39	2.11	4.33
		C_2H_6	2.79	1.03	–	–	–
	70	C_2H_4	1.88	0.817	1.89	1.2	3.41
		C_2H_6	2.63	0.817	–	–	–
8CuCl/CMK-3	30	C_2H_4	1.33	1.32	4.37	3.37	4.95
		C_2H_6	2.29	1.32	–	–	–
	50	C_2H_4	1.24	0.970	3.16	2.42	4.56
		C2H6	2.22	0.970	–	–	–
	70	C_2H_4	1.03	0.785	3.06	1.596	3.5
		C_2H_6	1.84	0.785	–	–	–

ethylene and ethane on CMK-3 evidences the similar interaction of both adsorbates with adsorbent. The heat of adsorption for ethylene is slightly higher than that for ethane, whereas the uptakes show an opposite tendency as described above. The difference in the size of ethylene and ethane as well as their adsorption geometry should be responsible for this phenomenon (44,45). Different from CMK-3, the heat of adsorption of ethylene is much higher than that of ethane on 4CuCl/CMK-3. Apparently, this is because of the dispersion of CuCl on the surface of carbon. For the adsorbent 8CuCl/CMK-3, the difference between the heat of adsorption of ethylene and ethane become even larger than that for 4CuCl/CMK-3. Moreover, the isosteric heats of adsorption are found to be higher for ethylene when compared to ethane over the entire adsorption coverage. For nonpolar ethane molecules, no specific interaction between ethane and adsorbent is present; only the nonspecific interactions (e.g., dispersion, repulsion, and polarization) can contribute to the total energy of adsorption (46). The unsaturated adsorbate firstly interacts with specific adsorption sites. Therefore, the isosteric heat of adsorption of unsaturated ethylene on CuCl/CMK-3 is highest initially and stats to decrease suggest the presence of surface heterogeneity. A great difference of heat of adsorption between ethylene and ethane on 8CuCl/CMK-3 indicates that the adsorbent is promising for application in ethylene/ethane separation. The enhanced affinity of the carbon material toward unsaturated compounds may provide an alternative for adsorption/separation in various systems.

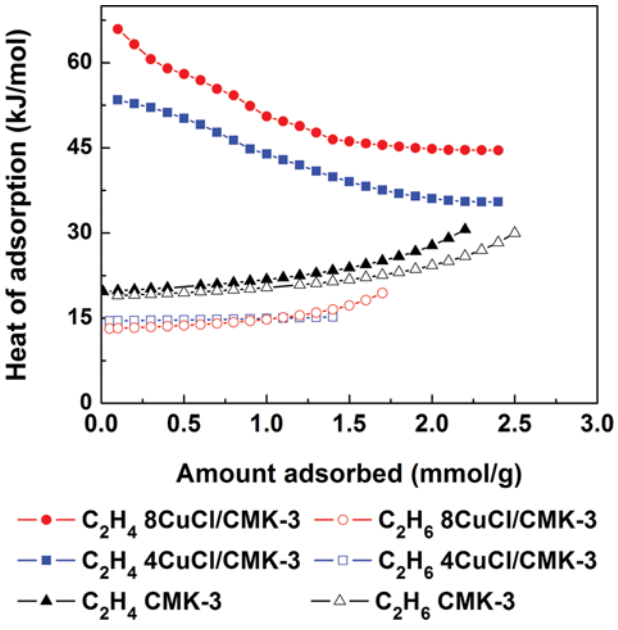

FIG. 8. Isosteric heat of adsorption of different samples as a function of adsorption amount. (Color figure available online)

CONCLUSIONS

Mesoporous carbon CMK-3 was used as support to load CuCl for π-complexation adsorption. Thermal treatment at 300°C for 4 h is proper to disperse CuCl and avoid the formation of metallic copper. Parent CMK-3 shows no selectivity toward the adsorption of ethylene over ethane.

The introduction of CuCl leads to an obvious improvement of ethylene/ethane selectivity, and the selectivity increases with the loading of CuCl. The adsorption isotherms can be well fitted with the corresponding models in spite of the adsorbents and adsorption temperatures. The fitting results, in combination with the heat of adsorption, demonstrate that the interaction of CuCl/CMK-3 with ethylene is apparently stronger than that with ethane.

ACKNOWLEDGEMENTS

We acknowledge the financial support for this work by the National Science Foundation of China (Nos. 20976082 and 21006048), the Major Basic Research Project of Natural Science Foundation of Jiangsu Province Colleges (No. 08KJA530001), the Specialized Research Fund for the Doctoral Program of Higher Education of China (No. 20093221120001), the Natural Science Foundation of Jiangsu Province Colleges (No. 09KJB530004), China Postdoctoral Science Foundation (No. 20110491406), the Research and Innovation Project for College Graduates of Jiangsu Province (Nos. CXZZ11_0350 and CXZZ12_0432), and the Priority Academic Program Development of Jiangsu Higher Education Institutions.

REFERENCES

1. Safarik, D.J.; Eldridge, R.B. (1998) Olefin/paraffin separations by reactive absorption: A review. *Ind. Eng. Chem. Res.*, 37: 2571.
2. Salleh, W.N.W.; Ismailab, A.F.; Matsuuraac, T.; Abdullaha, M.S. (2011) Selection and process conditions in the preparation of carbon membrane for gas separation: A review. *Sep. Purif. Rev.*, 40: 261.
3. Eldridge, R.B. (1993) Olefin/paraffin separation technology: A review. *Ind. Eng. Chem. Res.*, 32: 2208.
4. Li, J.R.; Sculley, J.; Zhou, H.C. (2011) Metal-organic frameworks for separation. *Chem. Rev.*, 112: 869.
5. Motelica, A.; Bruinsma, O.S.L.; Kreiter, R.; Exter, M.D.; Vente, J.F. (2012) Membrane retrofit option for paraffin/olefin separation-a technoeconomic evaluation. *Ind. Eng. Chem. Res.*, 51: 6977.
6. Pai, S.M.; Newalkar, B.L.; Choudary, N.V. (2009) Advances in Light Olefin Separation. *Petrotech-8th International Oil & Gas Conference and Exhibition*, 543.
7. Ruthven, D.M.; Reyes, S.C. (2007) Adsorptive separation of light olefins from paraffins. *Microporous Mesoporous Mater.*, 104: 59.
8. Grande, C.A.; Rodrigues, A.E. (2001) Adsorption equilibria and kinetics of propane and propylene in silica gel. *Ind. Eng. Chem. Res.*, 40: 1686.
9. Casado, C.; Bosque, J.; Navascués, N.; Téllez, C.; Coronas, J. (2009) Propane and 1, 3, 5-Triisopropylbenzene single gas adsorption on hollow silicalite-1 spheres. *Microporous Mesoporous Mater.*, 120: 69.
10. Aguilar, A.G.; Romero, P.Á. (2009) Adsorption of C_2H_4, C_2H_6 and CO_2 on cation-exchanged clinoptilolite. *Adsorpt. Sci. Technol.*, 27: 523.
11. Palomino, M.; Cantin, A.; Corma, A.; Leiva, S.; Rey, F.; Valencia, S. (2007) Pure silica ITQ-32 zeolite allows separation of linear olefins from paraffins. *Chem. Commun.*, 1233.
12. Li, K.H.; Olson, D.H.; Seidel, J.; Emge, T.J.; Gong, H.W.; Zeng, H.P.; Li, J. (2009) Zeolitic imidazolate frameworks for kinetic separation of propane and propene. *J. Am. Chem. Soc.*, 131: 10368.
13. Iucolano, F.; Aprea, P.; Caputo, D.; Colella, C.; Eic, M.; Huang, Q. (2008) Adsorption and diffusion of propane and propylene in Ag^+-Impregnated MCM-41. *Adsorption*, 14: 241.
14. Grande, C.A.; Gigola, C.; Rodrigues, A.E. (2002) Adsorption of propane and propylene in pellets and crystals of 5A zeolite. *Ind. Eng. Chem. Res.*, 41: 85.
15. Peng, J.; Ban, H.Y.; Zhang, X.T.; Song, L.J.; Sun, Z.L. (2005) Binary adsorption equilibrium of propylene and ethylene on silicalite-1: Prediction and experiment. *Chem. Phys. Lett.*, 401: 94.
16. Lamia, N.; Jorge, M.; Granato, M.A.; Paz, F.A.A.; Chevreau, H.; Rodrigues, A.E. (2009) Adsorption of propane, propylene and isobutane on a metal-organic framework: Molecular simulation and experiment. *Chem. Eng. Sci.*, 64: 3246.
17. Ko, C.H.; Han, S.S.; Park, J.H.; Cho, S.H.; Kim, J.N. (2006) Silver nitrate impregnated pellet-type adsorbents for propylene/propane separation. *Ind. Eng. Chem. Res.*, 45: 9129.
18. Takahashi, A.; Yang, R.T.; Munson, C.L.; Chinn, D. (2001) Cu(I)Y-zeolite as a superior adsorbent for diene/olefin separation. *Langmuir*, 17: 8405.
19. Choudary, N.V.; Kumar, P.; Bhat, T.S.G. (2002) Adsorption of light hydrocarbon gases on alkene-selective adsorbent. *Ind. Eng. Chem. Res.*, 41: 2728.
20. Padin, J.; Yang, R.T. (2000) New sorbents for olefin/paraffin separations by adsorption via π-complexation: Synthesis and effects of substrates. *Chem. Eng. Sci.*, 55: 2607.
21. Kargol, M.; Zajac, J.; Jones, D.J.; Steriotis, T.; Roziere, J.; Vitse, P. (2004) Porous silica materials derivatized with Cu and Ag cations for selective propene-propane adsorption from the gas phase: Aluminosilicate ion-exchanged monoliths. *Chem. Mater.*, 16: 3911.
22. Grande, C.A.; Araujo, J.D.P.; Cavenati, S.; Firpo, N.; Basaldella, E.; Rodrigues, A.E. (2004) New π-complexation adsorbents for propane-propylene separation. *Langmuir*, 20: 5291.
23. Khodakov, A.Y.; Zholobenko, V.L.; Bechara, R.; Durand, D. (2005) Impact of aqueous impregnation on the long-range ordering and mesoporous structure of cobalt containing MCM-41 and SBA-15 materials. *Microporous Mesoporous Mater.*, 79: 29.
24. Anson, A.; Wang, Y.; Lin, C.C.H.; Kuznicki, T.M.; Kuznicki, S.M. (2008) Adsorption of Ethane and Ethylene on Modified ETS-10. *Chem. Eng. Sci.*, 63: 4171.
25. Chen, L.; Liu, X.Q. (2008) π-Complexation mesoporous adsorbents Cu-MCM-48 for ethylene-ethane separation. *Chinese J. Chem. Eng.*, 16: 570.
26. He, Y.B.; Zhang, Z.J.; Xiang, S.C.; Fronczek, F.R.; Krishna, R.; Chen, B.L. (2012) A microporous metal-organic framework for highly selective separation of acetylene, ethylene, and ethane from methane at room temperature. *Chem. Eur. J.*, 18: 613.
27. Li, L.; Zhu, Z.H.; Lu, G.Q.; Yan, Z.F.; Qiao, S.Z. (2007) Catalytic ammonia decomposition over CMK-3 supported Ru catalysts: Effects of surface treatments of supports. *Carbon*, 45: 11.
28. Hussain, M.; Ihm, S.K. (2009) Synthesis, characterization, and hydrodesulfurization activity of new mesoporous carbon supported transition metal sulfide catalysts. *Ind. Eng. Chem. Res.*, 48: 698.
29. Sun, Y.; Liu, X.W.; Su, W.; Zhou, Y.P.; Zhou, L. (2007) Studies on ordered mesoporous materials for potential environmental and clean energy applications. *Appl. Surf. Sci.*, 253: 5650.
30. Zhou, H.; Zhu, S.; Honma, I.; Seki, K. (2004) Methane gas storage in self-ordered mesoporous carbon (CMK-3). *Chem. Phys. Lett.*, 396: 252.
31. Yu, L.; Zhao, C.X.; Long, X.; Chen, W. (2009) Ultrasonic synthesis and electrochemical characterization of V_2O_5/mesoporous carbon composites. *Microporous Mesoporous Mater.*, 126: 58.
32. Hartmann, M.; Vinu, A.; Chandrasekar, G. (2005) Adsorption of Vitamin E on mesoporous carbon molecular sieves. *Chem. Mater.*, 17: 829.

33. Liu, F.L.; Wang, J.H.; Li, L.Y.; Shao, Y.; Xu, Z.Y.; Zheng, S.R. (2009) Adsorption of direct yellow 12 onto ordered mesoporous carbon and activated carbon. *J. Chem. Eng. Data*, 54: 3043.
34. Vinu, A.; Streb, C.; Murugesan, V.; Hartmann, M. (2003) Adsorption of cytochrome C on new mesoporous carbon molecular sieves. *J. Phys. Chem. B*, 107: 8297.
35. He, J.G.; Ma, K.; Jin, J.; Dong, Z.P.; Wang, J.J.; Li, R. (2009) Preparation and characterization of octyl-modifed ordered mesoporous carbon CMK-3 for phenol adsorption. *Microporous Mesoporous Mater.*, 121: 173.
36. Lei, Z.B.; An, L.Z.; Dang, L.Q.; Zhao, M.Y.; Shi, J.Y.; Bai, S.Y.; Cao, Y.D. (2009) Highly dispersed platinum supported on nitrogen-containing ordered mesoporous carbon for methanol electrochemical oxidation. *Microporous Mesoporous Mater.*, 119: 30.
37. Zhao, D.Y.; Feng, J.L.; Huo, Q.S.; Melosh, N.; Fredrickson, G.H.; Chmelka, B.F.; Stucky, G.D. (1998) Triblock copolymer syntheses of mesoporous silica with periodic 50 to 300 angstrom pores. *Science*, 279: 548.
38. Jun, S.; Joo, S.H.; Ryoo, R.; Kruk, M.; Jaroniec, M.; Liu, Z.; Ohsuna, T.; Terasaki, O. (2000) Synthesis of new, nanoporous carbon with hexagonally ordered mesostructure. *J. Am. Chem. Soc.*, 122: 10712.
39. Yang, R.T.; Kikkinides, E.S. (1995) New sorbents for olefin/paraffin separations by adsorption via π-complexation. *AIChE J.*, 41: 509.
40. Valenzuela, D.P.; Myers, A.L. (1989) *Adsorption Equilibrium Data Handbook*; Prentice-Hall: New Jersey.
41. Li, Z.; Xie, K.C.; Slade, R.C.T. (2001) Studies of the interaction between CuCl and HY zeolite for preparing heterogeneous Cu^{I} catalyst. *Appl. Catal. A: Gen.*, 209: 107.
42. Xie, Y.C.; Tang, Y.Q. (1990) Spontaneous monolayer dispersion of oxides and salts onto surfaces of supports: applications to heterogeneous catalysis. *Adv. Catal.*, 37: 1.
43. Saini, V.K.; Andrade, M.; Pinto, M.L.; Carvalho, A.P.; Pires, J. (2010) How the Adsorption properties get changed when going from SBA-15 to its CMK-3 carbon replica. *Sep. Purif. Technol.*, 75: 366.
44. Peng, X.; Wang, W.C.; Xue, R.S.; Shen, Z.M. (2006) Adsorption separation of CH_4/CO_2 on mesocarbon microbeads: Experiment and modeling. *AIChE J.*, 52: 994.
45. Huang, H.Y.; Padin, J.; Yang, R.T. (1999) Comparison of π-complexations of ethylene and carbon monoxide with Cu^{+} and Ag^{+}. *Ind. Eng. Chem. Res.*, 38: 2720.
46. Basaldella, E.I.; Tara, J.C.; Armenta, G.A.; Iglesias, M.E.P. (2007) Cu/SBA-15 as adsorbent for propane/propylene separation. *J. Porous Mater.*, 14: 273.